Ultrasonics - Sonochemistry 43 (2018) 73–79

Contents lists available at ScienceDirect

Ultrasonics - Sonochemistry

journal homepage: www.elsevier.com/locate/ultson

Ultrasonic synthesis and characterization of poly(acrylamide)-*co*-poly (vinylimidazole)@MWCNTs composite for use as an electrochemical material

Won-Yong Jeon[a,b], Young-Bong Choi[a], Hyug-Han Kim[a,*]

[a] Department of Chemistry, College of Natural Science, Dankook University, Anseo-Dong, Cheonan, Chungnam 31116, Republic of Korea
[b] Department of Nanobiomedical Sciences and BK21 PLUS NBM Global Research Center for Regenerative Medicine, Dankook University, Anseo-Dong, Cheonan, Chungnam 31116, Republic of Korea

ARTICLE INFO

Keywords:
Biosensor
Glucose oxidase
MWCNTs
Hydrophilic polymer
Ultrasonic synthesis

ABSTRACT

Applying a nanocomposite to increase the conductivity of an electrode can facilitate electrochemical analysis. In this regard, multi-walled carbon nanotubes (MWCNTs) evenly dispersed in hydrophilic solution can play an important role in electrochemical bio-sensing due to their unique properties, such as their high electrical conductivity and ability to conjugate with hydrophilic enzymes. Herein, we report the simple ultrasonic synthesis of a highly dispersible, enzyme-binding nanocomposite, poly(acrylamide)-*co*-poly(vinyl imidazole) (7:1 mol ratio)-MWCNTs (PAA-PVI@MWCNTs). This material, having a zeta potential of 36.6 ± 0.53 mV, was applied as a film to an electrode surface and stably bound with glucose oxidase to transfer an electron between the enzyme and electrode in the presence of glucose. The PAA-PVI@MWCNTs composite, which was readily dispersed in deionized water, can be used as a biocompatible material for applications such as bio-sensing, point-of-care testing (POCT), and other health care functions.

1. Introduction

Electrochemical biosensors recognize electrical signals generated through biological reactions between an analyte and electrode, and have been exploited for both quantitative and qualitative analyses. The materials and components of the electrode are very important for measuring biological analytes [1,2], and many highly sensitive and reproducible materials have been investigated [3–6]. The carbon allotropes, encompassing fullerenes, CNTs and graphene, having remarkable properties has been studying due to their extraordinary structure and rigorous surface dimensionality [7–9]. Multi-walled carbon nanotubes (MWCNTs), with their excellent electrical conductivity, high surface area, good corrosion resistance, and unique chemical, physical, and mechanical properties, have been applied in electrochemical biosensing materials due to their controllable properties with various biomolecule. However, MWCNTs are difficult to use directly for biological systems because of their hydrophobicity and insolubility [6,10,11]. Therefore, many researchers have developed MWCNTs dispersion methods, having biocompatibility and high dispersion, using chemical and physical functionalization [12–16].

One typical chemical functionalization method uses nitric or sulfuric acid to introduce carboxylic acid groups onto the MWCNTs, which modifies the sp^2 surface of the MWCNTs to an sp^3 hybridized structure. Although chemically functionalized MWCNTs are more hydrophilic because of their surface carboxylic acids [17–19], their electrical conductivity is reduced due to the destruction of their sp^2 structure (π electrons). Further disadvantages of this approach are the requirements for extreme sonication, the environmentally unfriendly use of strong acids, and a complex washing step to remove residual acid from the product [20]. In another chemical MWCNTs functionalization method, non-ionic, anionic, and cationic surfactants having both hydrophilic and hydrophobic structural components have been employed [21–23]. However, these reagents can alter the properties of the MWCNTs and the residual surfactant can be difficult to remove. Physical functionalization methods have also been developed, as exemplified by the wrapping of the MWCNTs surface with polymers such as poly(phenylene vinylene) [24] or polystyrene [25]. Polymer chains that contain aromatic rings can be wrapped onto MWCNTs through van der Waals interactions and π-π stacking [24–26]. However, MWCNTs composites with polymers having only aromatic rings cannot be dispersed in

Abbreviations: GOx, glucose oxidase; ITO, indium tin oxide; PAA, poly(acrylamide); PVI, poly(vinylimidazole

* Corresponding author at: 213 Analysis Chemistry Laboratory, Department of Chemistry, College of Natural Science, Dankook University, Anseo-Dong, Cheonan, Chungnam 31116, Republic of Korea.
E-mail address: hankim@dankook.ac.kr (H.-H. Kim).

https://doi.org/10.1016/j.ultsonch.2017.11.024
Received 30 August 2017; Received in revised form 17 November 2017; Accepted 17 November 2017
Available online 21 November 2017

aqueous solution. So, MWCNTs dispersions prepared with hydrophilic polymers such as poly(acrylamide)-*co*-poly(sodium methacrylate) [27], poly(methacrylic acid-*co*-acrylamide) [28], poly(acrylamide) [29], and poly(*N,N*-dimethylacrylamide) [30] have been developed, affording inexpensive and soluble materials for engineering applications. The hydrophilic polymer, poly(acrylamide)-*co*-poly(vinylimidazole) (PAA-PVI), has been studied as an electrochemical biosensor material due to its water-soluble nature [31–35].

The ultrasound as a green, inexpensive, express, and convenient technology have widely used for the homogeneous dispersion of MWCNTs with polymer. When an ultrasonic wave, which have cycles of compression and expansion, passes through a liquid, compression cycles exert a positive pressure on the liquid, pushing the molecules together; expansion cycles exert a negative pressure, pulling the molecules away from one another. A sound wave of sufficient intensity can create cavities in the liquid during the negative pressure. These cavities grow and enlarge over many cycles. At the end of the cavitation cycle; the collapse of microbubbles produces transient micro hot spots with temperature and pressure that are much upper than that of the surrounding liquid. Also, these irradiations provide the necessary thermal energy to react and increase the collision frequency of nanofiller and polymer matrix to form new intermolecular H-bonding between the MWCNTs and the polymer. Therefore, to achieve a very high homogeneous dispersed MWCNTs with polymer, an ultrasonic method is suitable [36,37].

Sensing systems to detect glucose have been classified into three generations. First-generation glucose sensors measure production of the hydrogen peroxide by glucose oxidase from oxygen, hydrogen, and glucose. Second-generation glucose sensors use a mediator which transfers an electron faster than oxygen from an enzyme to the electrode. Finally, third-generation glucose sensors detect the electron from glucose directly without a mediator (i.e., the enzyme is “wired” to the electrode). Glucose oxidase (GOx) is commonly used to detect glucose directly, and has been wired onto electrodes through metal nanoparticles, conducting polymers, and carbon-based materials (graphene, single-walled CNTs (SWCNTs), and MWCNTs) [38–41]. The co-factor redox peak for the electrode-wired GOx is around −0.332 V (versus Ag/AgCl reference) [42]. To directly detect glucose, therefore, it would be desirable to use water-soluble MWCNTs to adsorb the enzyme co-factor on the sensor electrode.

In this work, we synthesized hydrophilic PAA-PVI@MWCNTs via simple ultrasonic method. The physicochemical, morphological, and electrochemical characteristics of PAA-PVI and its MWCNTs composite were investigated. Finally, adsorption of the GOx enzyme onto a prepared PAA-PVI@MWCNTs/indium tin oxide (ITO) electrode was evaluated, and the resultant biosensor was examined for the determination of glucose and as a high electron-transfer material.

2. Experimental

2.1. Materials

Multi-walled carbon nanotubes (Model MR99, > 99 wt%, 5–15 nm diameter, ~20 μm length) were purchased from Carbon Nano-material Technology Co. (Pohang, Korea). Acrylamide, 1-vinylimidazole, *N,N,N′,N′*-tetramethylethylenediamine, poly(ethylene glycol) diglycidyl ether (PEGDGE), and ammonium persulfate were purchased from Sigma-Aldrich Co. (Milwaukee, WI, USA). Glucose oxidase (GOx; 219 U/mg) from *Aspergillus Niger* was purchased from Amano Enzyme Inc. (Japan). Phosphate-buffered saline (PBS, 4.3 mM NaH_2PO_4, 15.1 mM Na_2HPO_4, and 140 mM NaCl) and all other solutions were prepared using deionized Milli-Q (DI) water (Millipore, Japan). A Powersonic 510 ultrasonic bath (Hwashin Tech, Korea) was used for the ultrasonic synthesis of PAA-PVI@MWCNTs.

2.2. Preparation of PAA-PVI (7:1) and PAA-PVI@MWCNTs

The hydrophilic PAA-PVI (7:1) polymer was synthesized by minor modification of the reported method [43]. Acrylamide (4.967 g, 0.07 mol) and 1-vinylimidazole (0.905 mL, 0.01 mol) were dissolved in DI water (150 mL) in a 250 mL beaker with vigorous stirring. A mixed solution of ammonium persulfate (0.2 g) and *N,N,N′,N′*-tetramethylethylenediamine (0.21 mL) in DI water (30 mL) was added dropwise over 30 min to the monomer solution in the beaker at 40 °C with vigorous stirring. Then, the solution was added dropwise into acetone (500 mL) to precipitate the synthesized polymer. The hydrophilic PAA-PVI polymer was vacuum dried for 1 day in a desiccator after filtration. The white powder was assessed by Fourier transform infrared spectroscopy (FT-IR; Frontier & Spotlight 400, PerkinElmer, USA). PAA-PVI (1.667 mg) was completely dissolved in DI water (5 mL). Then, the MWCNTs (5 mg) were added, and the mixture was sonicated at 40 kHz and 50 °C for 2 h. Herein, the ultrasonic method was provide for interaction between the MWCNTs and PAA-PVI polymer. The ultrasonic method have been lead to achieve a very high homogeneity and obtain clear solution. The PAA-PVI@MWCNTs dispersion was characterized in terms of its physicochemical, morphological, and electrochemical properties (Scheme 1).

2.3. Characterization of PAA-PVI and PAA-PVI@MWCNTs

The physicochemical and morphological properties of the MWCNTs, acrylamide, 1-vinylimidazole, PAA-PVI (7:1), and PAA-PVI@MWCNTs composite were examined by zeta potential analysis (SZ-100 nanoparticle analyzer, Horiba, Japan), FT-IR (PerkinElmer), raman spectroscopy (LabRAM HR Evolution, Horiba, Paris, France), X-ray photoelectron spectroscopy (XPS, SPECS, Berlin, Germany), thermogravimetric analysis (TGA, Rigaku, Japan), high-resolution transmission electron microscopy (HR-TEM, JEOL, Japan), and electrochemical analysis (CHI 660B workstation, CH Instruments, Austin, TX, USA).

2.4. Fabrication of enzyme electrode

Indium tin oxide (ITO) electrodes were cleaned by immersion in piranha solution (H_2O_2:H_2SO_4 = 3:1, v/v) for 5 mins. The ITO electrodes sonicated for 5 mins in DI water and dried completely under a stream of nitrogen gas at room temperature. Prepared PAA-PVI@MWCNTs (40 μL, 1 mg/mL in DI water) was cast onto a cleaned ITO electrode and then dried for 12 h at room temperature. The 40 μL mixed solutions of GOx (40 mg/mL in PBS, volume, ratio 4) and PEGDGE (10 mg/mL in DW, volume, ratio 1) were loaded onto the PAA-PVI@MWCNTs/ITO electrode, and then dried for 12 h at room temperature. The fabricated GOx/PAA-PVI@MWCNTs/ITO electrode was stored at 4 °C in the refrigerator before use in the determination of glucose as a third-generation biosensor material.

2.5. Biosensing apparatus and electrodes

A GOx/PAA-PVI@MWCNTs/ITO electrode (6.0 mm diameter) was used as the working electrode, and a micro Ag/AgCl (3.0 M KCl, Cypress, Lawrence, KS, USA) scrolled with a 0.5 mm diameter platinum wire was used as the reference and counter electrode, respectively. Electrochemical impedance spectroscopy (EIS) measurements of the modified electrodes were collected in 0.5 M KCl (pH = 7.4) solution containing 2.0 mM $K_3[Fe(CN)_6]/K_4[Fe(CN)_6]$ at 0.266 V (vs. Ag/AgCl). The amplitude was 5 mV and the frequency range was 1–10,000 Hz. The electrical glucose responses in the GOx/PAA-PVI@MWCNTs/ITO electrode were measured by cyclic voltammetry (CV) under oxygen-saturated conditions. CV experiments were performed to investigate the electron-transfer rate constant and the response to different glucose concentrations (0, 1, 5, 8, 10 and 20 mM). The glucose concentration

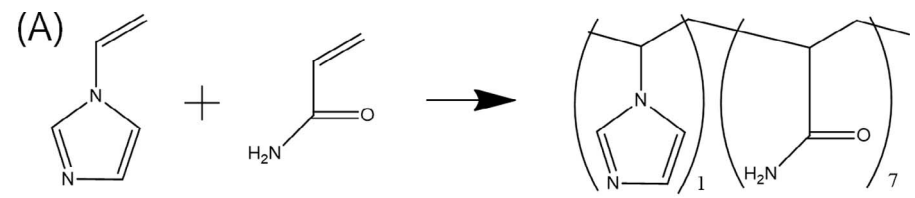

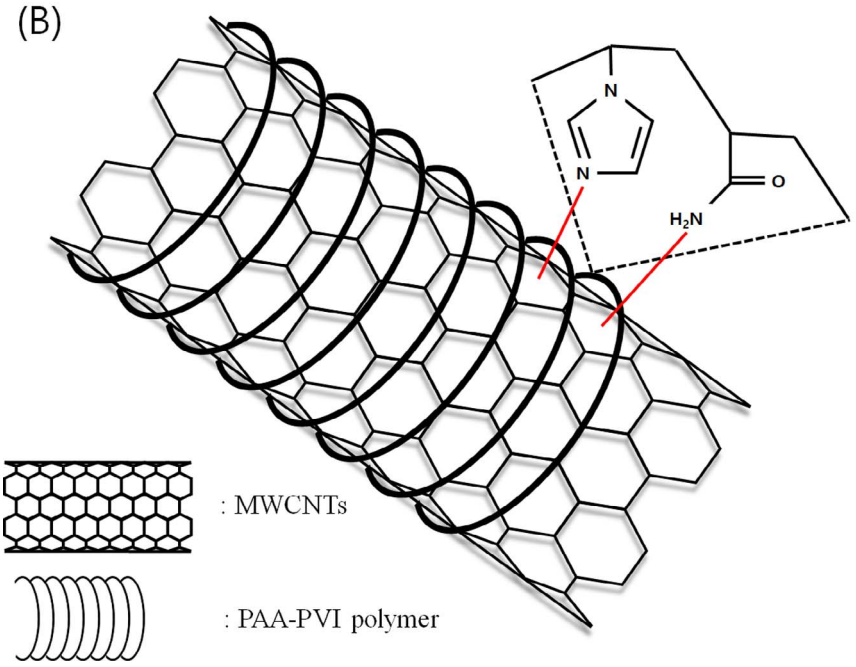

Scheme 1. Schematic of (A) synthesized PAA-PVI polymer and (B) PAA-PVI composited with MWCNTs.

curve results were collected at −0.408 V vs. Ag/AgCl.

3. Results and discussion

3.1. Chemical properties of PAA-PVI

The structure of the co-polymerized acrylamide and 1-vinylimidazole was assessed by FT-IR (Fig. 1). The FT-IR spectrum of PAA-PVI (line) shows the disappearance of specific peaks due to the vinyl and acrylate groups in 1-vinylimidazole (dash) and acrylamide (dot), such as the weak = CH_2 antisymmetric stretch at 3102 cm^{-1}, medium = CH_2 rocking band at 1051 cm^{-1}, and strong = CH_2 wag at 962 cm^{-1}. These results confirm successful co-polymerization to PAA-PVI [44–47].

3.2. Physicochemical and morphological characterization of PAA-PVI@MWCNTs

Fig. 2a presents a photograph of the highly dispersed state of the PAA-PVI composited with MWCNTs in DI water after centrifuging for 1 h at 13,000 rpm. The morphology of the composite was observed by HR-TEM (Fig. 2b), which reveals a uniform PAA-PVI polymer layer with a thickness of 3.08 nm on the MWCNTs surface. The FT-IR spectra for PAA-PVI@MWCNTs (line), PAA-PVI (dash), and the MWCNTs (dot) are shown in Fig. 2c. In the spectrum of PAA-PVI@MWCNTs, the imidazole ring stretching and NH bending bands at 1450 and 1500 cm^{-1}, respectively, are decreased compared to the pristine PAA-PVI. These results suggest that the imidazole and amide moieties of the PAA-PVI have stacked with the MWCNTs through cationic π-π interactions, similarly to the previously published catecholamine effect [48]. The TGA results for PAA-PVI@MWCNTs (line), PAA-PVI (dash), and MWCNTs

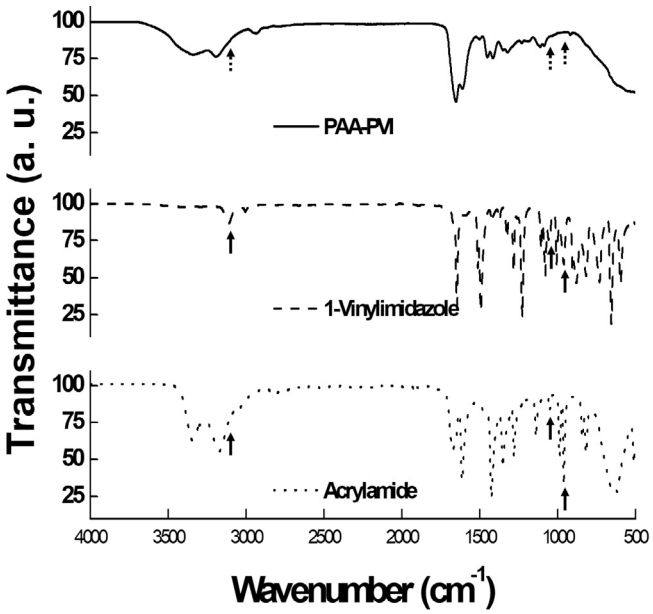

Fig. 1. FT-IR spectra of PAA-PVI polymer (line), 1-vinylimidazole (dash), and acrylamide (dot).

(dot) in Fig. 2d reveal a major mass loss of the MWCNTs indicated over the temperature range of 600–800 °C. And the PAA-PVI polymer decomposed at the range of 200–400 °C. However, the polymer (line) in PAA-PVI@MWCNTs decomposed slowly (500–700 °C) than original PAA-PVI (dash). The result shown that the PAA-PVI polymer well composited in MWCNTs. Zeta potential measurements numerically

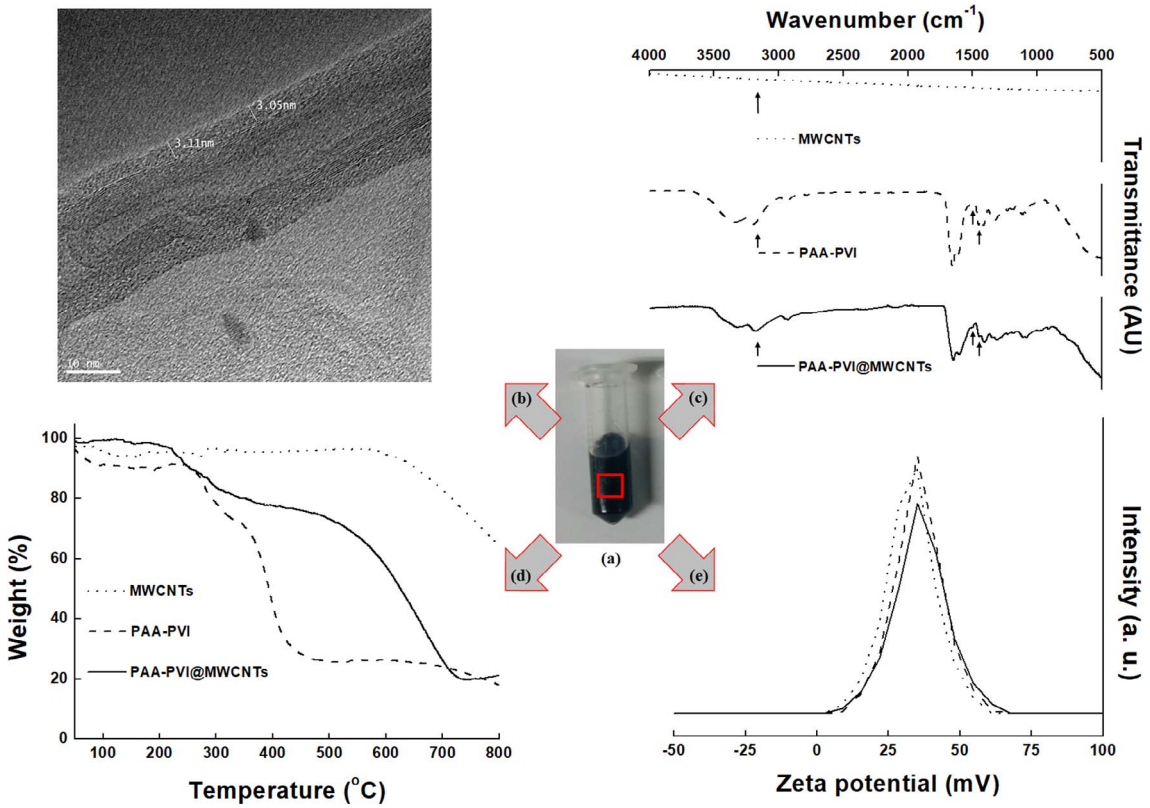

Fig. 2. (a) Photograph of PAA-PVI@MWCNTs after centrifuging. (b) HR-TEM image, (c) FT-IR spectra, (d) TGA traces, and (e) zeta potential measurements of the composite and its components.

indicate the dispersion state of a solution. Previous studies showed that the zeta potential for poly(ethyleneimine), which has a terminal amine functional group, was positive, and that for sodium dodecyl sulfate (SDS), which has a terminal acrylic acid functional group, was negative. Also, an increasing SDS content (with its negative terminal functional groups) showed increasing zeta potential values [49–51]. The average zeta potential of the prepared PAA-PVI@MWCNTs (7:1 mol ratio) is 36.6 ± 0.53 mV (Fig. 2e), and its positive value may be attributed to the positive amide functional groups of the PAA-PVI. The zeta potentials for MWCNTs composites prepared using different PAA-PVI ratios are shown in Fig. S1 and Table S1. And qualitative data of PAA-PVI composited MWCNTs are shown in Fig. S2.

In order to raman spectroscopy, the typical MWCNTs has observed D band and G band around at 1350 cm^{-1} and 1583 cm^{-1} respectively [52]. The D band and G band of our MWCNTs (dot) show the bands at 1350.68 cm^{-1} and 1583.13 cm^{-1}in Fig. 3. And the synthesized PAA-PVI polymer (dash) show the bands of 1622.91 cm^{-1}. The D band and G band of PAA-PVI@MWCNTs (line) showed the peaks of 1352.39 cm^{-1} and 1591.43 cm^{-1} respectively. This result suggest that PAA-PVI polymer coated well onto the surface of MWCNTs. Also, the ratio of D band and G band is important for checking defect of MWCNTs [53]. As shown MWCNTs (dot) and PAA-PVI@MWCNTs (line) of Fig. 3, there is no defect despite the use of ultrasonic wave.

The XPS spectra of PAA-PVI@MWCNTs, PAA-PVI, and MWCNTs were shown in Fig. 4. The XPS spectra at sp^2 hybridized carbon (C=C) of MWCNTs is generally known to have the binding energy as 284.6 eV [54]. The XPS data of our MWCNTs (dot) showed 284.59 eV as C=C binding energy. And the main C=C peak of PAA-PVI@MWCNTs (line) was shifted to 283.85 eV. The result data suggest that PAA-PVI polymer effected to C=C binding energy by composited onto surface of MWCNTs [55].

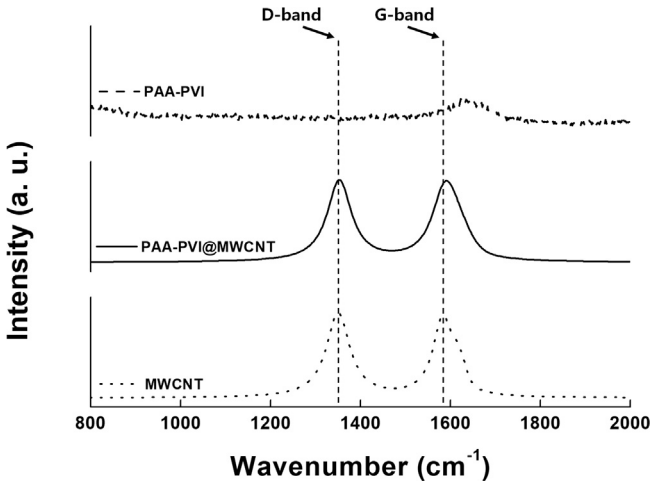

Fig. 3. Raman spectra of MWCNTs (dot), PAA-PVI (dash), and PAA-PVI@MWCNTs (line).

3.3. Electrochemical characterization of modified electrodes

The interface properties of the modified electrodes were studied by EIS and CV (Fig. 5). In a Nyquist plot of EIS data, the semicircular part at higher frequencies corresponds to an electron-transfer-limited process, and the linear part at lower frequencies corresponds to a diffusion-controlled process. The semicircle diameter indicates the electron-transfer resistance (R_{et}) [56]. The impedance spectra of the bare ITO, PAA-PVI/ITO, MWCNTs/ITO, and PAA-PVI@MWCNTs/ITO electrodes were investigated in 0.5 M KCl (pH = 7.4) solution containing 2.0 mM $K_3[Fe(CN)_6]/K_4[Fe(CN)_6]$. As shown in Fig. 5a, the R_{et} of PAA-PVI/ITO (b, black square) dramatically increases over that of bare ITO (a, white inverted triangle), from 211 to 675 Ω, and the R_{et} of PAA-PVI@MWCNTs/ITO (d, white triangle) slowly declines from that of

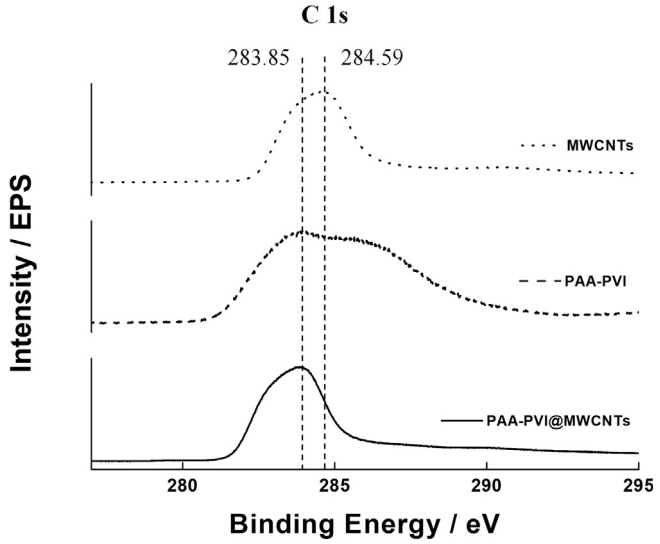

Fig. 4. XPS spectra of MWCNTs (dot), PAA-PVI (dash), and PAA-PVI@MWCNTs (line) in C 1s region.

MWCNTs/ITO (c, black circle) (from 98.7 to 59.3 Ω). Thus, while films of the PAA-PVI polymer increase R_{et} on the ITO surface, the PAA-PVI@MWCNTs composite film can more promote electron transfer at the surface of the ITO electrode than MWCNTs. The CV results in Fig. S3 support the EIS data.

These electrodes were also used to evaluate the redox potential of GOx. The redox potential of the GOx co-factor is observed in the GOx-modified PAA-PVI@MWCNTs/ITO electrode (dash dot) only (Fig. 5b), which verifies that hydrophilic PAA-PVI@MWCNTs can be wired with GOx to transfer electrons from the redox co-factor of the enzyme to the surface of the ITO electrode. The other modified electrodes [GOx/ITO (line), GOx/PAA-PVI/ITO (dash), and GOx/MWCNTs/ITO (dot)] exhibit no redox peak for the enzyme. Fig. 6a shows the CVs of the GOx/PAA-PVI@MWCNTs/ITO electrode at pH 7.4 for different scan rates. The peak currents during both oxidation and reduction are linearly proportional to the scan rate in the range of 0.05–2 V/s. The electron-transfer rate constant (k_s) for the GOx/PAA-PVI@MWCNTs/ITO electrode was calculated from the dependence of the peak-to-peak separation (ΔE_p) at different scan rates using the Laviron equation (Fig. 6b) [57]. A charge transfer coefficient (α) of 0.48 and k_s of 8.195/s are obtained. This k_s value is much larger than values obtained for other polymer–MWCNTs composites [58,59]. Therefore, the PAA-PVI polymer-based MWCNTs can provide a good environment for the GOx co-factor and facilitate the electron-transfer reaction. This may be a result of the wiring between the GOx co-factor and the MWCNTs by the hydrophilic PAA-PVI polymer.

3.4. Application of GOx/PAA-PVI@MWCNTs/ITO for direct glucose sensing

The CV technique was used to measure various concentrations of glucose. Fig. 7a presents the sensor responses to different concentrations of glucose under oxygen-saturated conditions. The data were collected at −0.408 V vs. Ag/AgCl. The cathodic peak of GOx increases with successive increases in the glucose concentration (0, 1, 5, 8, 10 and 20 mM). As shown in Fig. 7b, the reduction peak current decreases with increasing glucose concentration. The amount of glucose is determined by monitoring the decrease in the reduction peak current on the GOx/PAA-PVI@MWCNTs/ITO electrode. The linearity range is from 0 to 10 mM of glucose with a correlation coefficient of 0.971. The limit of detection (LOD) is 0.4 mM, with a relative standard deviation (RSD) of 3.88% ($N = 4$, where N denotes the number of different electrodes used). Therefore, the PAA-PVI/ MWCNTs-based electrode with GOx can be used for the determination of glucose. These results indicate that PAA-PVI@MWCNTs can be used as a biomaterial in biosensor applications.

4. Conclusions

We prepared and characterized a PAA-PVI@MWCNTs composite by the simple, safe, and rapid sonication of PAA-PVI with MWCNTs, avoiding the problems of other hazardous functionalization methods involving strong acids. The synthesized PAA-PVI serves to form a well-dispersed MWCNTs suspension as well as immobilize the GOx enzyme. After its adsorption onto an ITO substrate and wiring with GOx, we investigated the newly fabricated biosensor's ability to detect glucose using the direct electron-transfer reaction of the GOx co-factor at the GOx/PAA-PVI@MWCNTs/ITO electrode. Glucose was satisfactorily detected by the GOx/PAA-PVI@MWCNTs/ITO electrode, displaying a linear response in the range of 0–10 mM glucose with an LOD of 0.4 mM and an RSD of 3.88%. The simple ultrasonic synthesis method developed here to disperse the MWCNTs may offer a new approach for developing novel types of highly sensitive electrochemical biosensors.

Acknowledgement

Following are results of a study on the "Leades in INdustry-university Cooperation" Project, supported by the Ministry of Education and National Research Foundation (R-2016-00675) of Korea. And it was supported in part by the Basic Science Research Program through the National Research Foundation of Korea (NRF), funded by the Ministry of Education (2017R1A63A11035249).

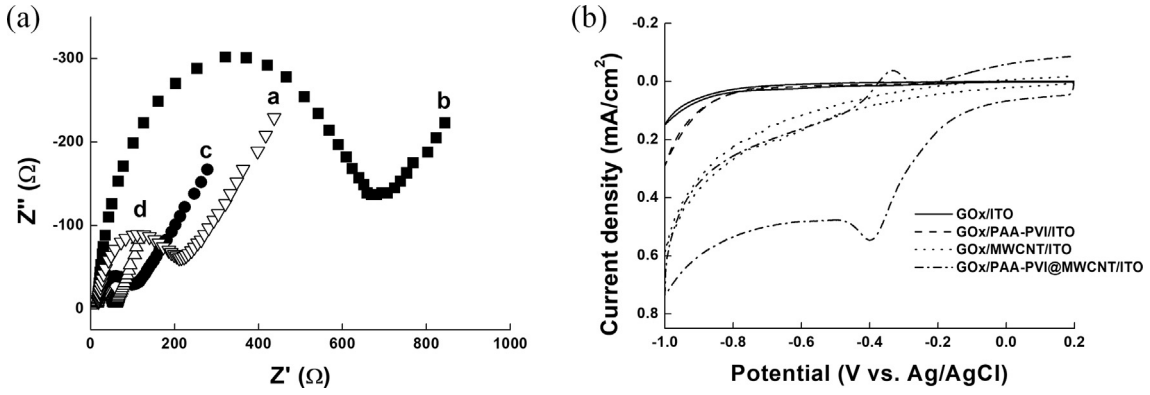

Fig. 5. (A) EIS spectra of (a) bare ITO, (b) PAA-PVI/ITO, (c) MWCNTs/ITO, and (d) PAA-PVI@MWCNTs/ITO electrodes in the frequency range of 1 to 10^4 Hz in 0.5 M KCl (pH = 7.4) containing 2.0 mM $K_3[Fe(CN)_6]/K_4[Fe(CN)_6]$. (B) Cyclic voltammograms of differently GOx-modified electrodes at a scan rate of 50 mV/s in 0.1 M PBS (pH = 7.4).

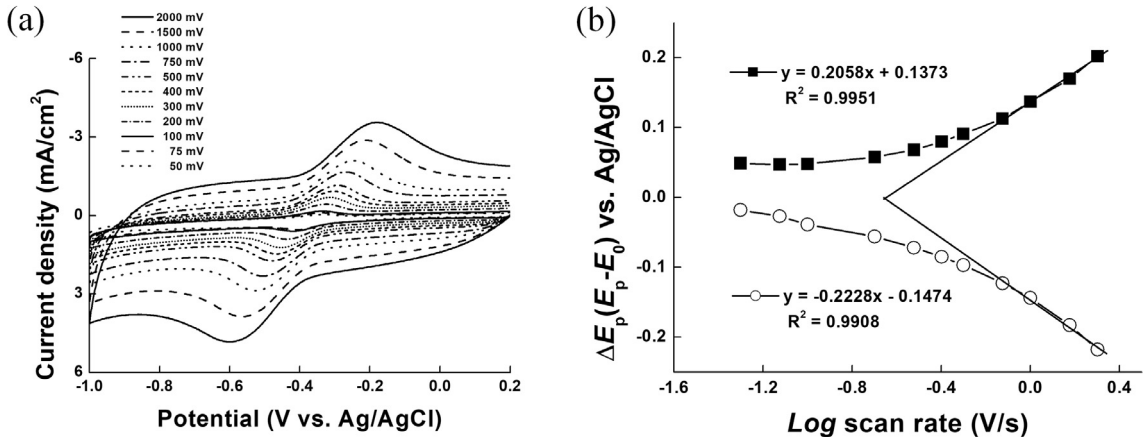

Fig. 6. (a) Cyclic voltammograms and (b) peak potential separations vs. log (scan rate) for the GOx/PAA-PVI@MWCNTs/ITO electrode.

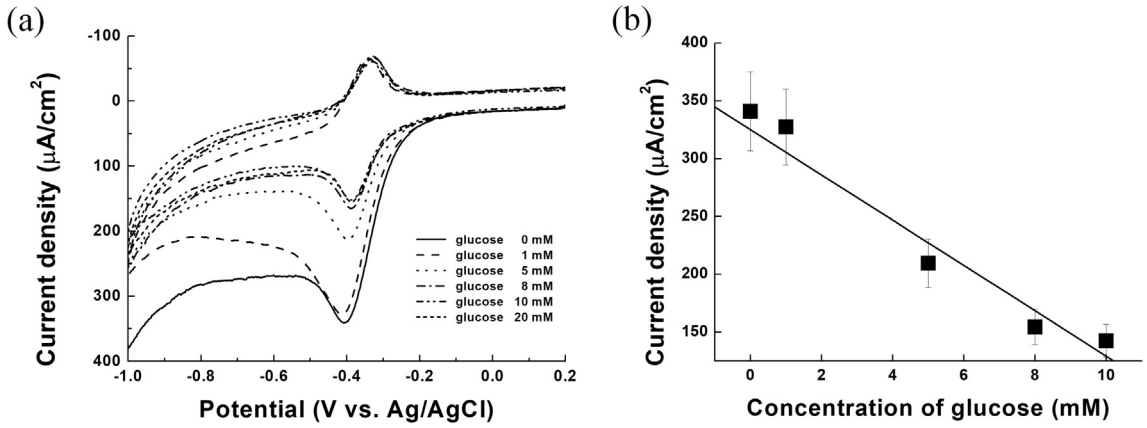

Fig. 7. Electrochemical measurements for glucose on GOx/PAA-PVI@MWCNTs/ITO electrode: (a) Cyclic voltammograms and (b) calibration curve for the anodic current at −0.408 V vs. Ag/AgCl.

Appendix A. Supplementary data

Supplementary data associated with this article can be found, in the online version, at http://dx.doi.org/10.1016/j.ultsonch.2017.11.024.

References

[1] J. Wang, Electrochemical glucose biosensors, Chem, Rev. 108 (2008) 814–825.
[2] D. Grieshaber, R. Mackenzie, J. Vörös, E. Reimhult, Electrochemical biosensors-sensor principles and architectures, Sensors 8 (2008) 1400–1458.
[3] F.T.C. Moreira, R.A.F. Dutra, J.P.C. Noronha, M.G.F. Sales, Electrochemical biosensor based on biomimetic material for myoglobin detection, Electrochim. Acta 107 (2013) 481–487.
[4] B.K. Jena, C.R. Raj, Electrochemical biosensor based on integrated assembly of dehydrogenase enzymes and gold nanoparticles, Anal. Chem. 78 (2006) 6332–6339.
[5] M. Pumera, A. Ambrosi, A. Bonanni, E.L.K. Chng, H.L. Poh, Graphene for electrochemical sensing and biosensing, Trends Anal. Chem. 29 (2010) 954–965.
[6] J. Wang, M. Musameh, Carbon nanotube/teflon composite electrochemical sensors and biosensors, Anal. Chem. 75 (2003) 2075–2079.
[7] R.P. Deo, J. Wang, I. Block, A. Mulchandani, K.A. Joshi, M. Trojanowicz, F. Scholz, W. Chen, Y. Lin, Determination of organophosphate pesticides at a carbon nanotube/organophosphorus hydrolase electrochemical biosensor, Anal. Chim. Acta 530 (2005) 185–189.
[8] S.S. Maktedar, G. Avashthi, M. Singh, Understanding the significance of O-doped graphene towards biomedical applications, RSC Adv. 115 (2016) 114264–114275.
[9] S.S. Maktedar, G. Avashthi, M. Singh, Ultrasound assisted simultaneous reduction and direct functionalization of graphene oxide with thermal and cytotoxicity profile, Ultrason. Sonochem. 34 (2017) 856–864.
[10] S.S. Maktedar, P. Malik, G. Avashthi, M. Singh, Dispersion enhancing effect of sonochemically functionalized graphene oxide for catalyzing antioxidant efficacy of curcumin, Ultrason. Sonochem. 39 (2017) 208–217.
[11] J.C. Claussen, A.D. Franklin, A. Haque, D.M. Porterfield, T.S. Fisher, Electrochemical biosensor of nanocube-augmented carbon nanotube networks, ACS Nano 3 (2009) 37–44.
[12] A. Amiri, H.Z. Zardini, M. Shanbedi, M. Maghrebi, M. Baniadam, B. Tolueinia, Efficient method for functionalization of carbon nanotubes by lysine and improved antimicrobial activity and water-dispersion, Mater. Lett. 72 (2012) 153–156.
[13] F. Zhang, H. Zhang, Z. Zhang, Z. Chen, Q. Xu, Modification of carbon nanotubes: water-soluble polymers nanocrystal wrapping to periodic patterning with assistance of supercritical CO_2, Macromolecules 41 (2008) 4519–4523.
[14] F. Avilés, J.V. Cauich-Rodríguez, L. Moo-Tah, A. May-Pat, R. Vargas-Coronado, Evaluation of mild acid oxidation treatments for MWCNT functionalization, Carbon 47 (2009) 2970–2975.
[15] M. Zhang, L. Su, L. Mao, Surfactant functionalization of carbon nanotubes (CNTs) for layer-by-layer assembling of CNT multi-layer films and fabrication of gold nanoparticle/CNT nanohybrid, Carbon 44 (2006) 276–283.
[16] A.G. Osorio, I.C.L. Silveira, V.L. Bueno, C.P. Bergmann, H_2SO_4/HNO_3/HCl—functionalization and its effect on dispersion of carbon nanotubes in aqueous media, Appl. Surf. Sci. 255 (2008) 2485–2489.
[17] P.C. Ma, N.A. Siddiqui, G. Marom, J.K. Kim, Dispersion and functionalization of carbon nanotubes for polymer-based nanocomposites: a review, Composites Part A 41 (2010) 1345–1367.
[18] K. Esumi, M. Ishigami, A. Nakajima, K. Sawada, H. Honda, Chemical treatment of carbon nanotubes, Carbon 34 (1996) 279–281.
[19] V. Datsyuk, M. Kalyva, K. Papagelis, J. Parthenios, D. Tasis, A. Siokou, I. Kallitsis, C. Galiotis, Chemical oxidation of multiwalled carbon nanotubes, Carbon 46 (2008) 833–840.
[20] P. Kar, A. Choudhury, Carboxylic acid functionalized multi-walled carbon nanotube doped polyaniline for chloroform sensors, Sens. Actuators, B 183 (2013) 25–33.
[21] X. Gong, J. Liu, S. Baskaran, R.D. Voise, J.S. Young, Surfactant-assisted processing of carbon nanotube/polymer composites, Chem. Mater. 12 (2000) 1049–1052.
[22] M.F. Islam, E. Rojas, D.M. Bergey, A.T. Johnson, A.G. Yodh, High weight fraction surfactant solubilization of single-wall carbon nanotubes in water, Nano Lett. 3 (2003) 269–273.
[23] E.A. Whitsitt, A.R. Barron, Silica coated single walled carbon nanotubes, Nano Lett. 3 (2003) 775–778.
[24] B. McCarthy, J.N. Coleman, R. Czerw, A.B. Dalton, D.L. Carroll, W.J. Blau, Microscopy studies of nanotube-conjugated polymer interactions, Synth. Met. 121 (2001) 1225–1226.
[25] D.E. Hill, Y. Lin, A.M. Rao, L.F. Allard, Y.P. Sun, Functionalization of carbon nanotubes with polystyrene, Macromolecules 35 (2002) 9466–9471.
[26] V. Goornavar, R. Jeffers, S. Biradar, G.T. Ramesh, Utilization of highly purified

single wall carbon nanotubes dispersed in polymer thin films for an improved performance of an electrochemical glucose sensor, Mater. Sci. Eng., C 40 (2014) 299–307.
[27] Z. Liu, Z. Yang, Y. Luo, Swelling, pH sensitivity, and mechanical properties of poly (acrylamide-co-sodium methacrylate) nanocomposite hydrogels impregnated with carboxyl-functionalized carbon nanotubes, Polym. Compos. 33 (2012) 665–674.
[28] K. Zhan, H. Liu, H. Zhang, Y. Chen, H. Ni, M. Wu, D. Sun, Y. Chen, A facile method for the immobilization of myoglobin on multi-walled carbon nanotubes: poly (methacrylic acid-co-acrylamide) nanocomposite and its application for direct bio-detection of H_2O_2, J. Electroanal. Chem. 724 (2014) 80–86.
[29] J.H. Hong, C.K. Hong, S.J. Choe, S.E. Shim, Preparation of poly (acrylamide)/MWNTs nanocomposite using carboxylated MWNTs, J. Polym. Sci., Part A: Polym. Chem. 45 (2007) 3477–3481.
[30] D. Shao, X. Ren, J. Hu, Y. Chen, X. Wang, Preconcentration of Pb^{2+} from aqueous solution using poly (acrylamide) and poly (N, N-dimethylacrylamide) grafted multiwalled carbon nanotubes, Colloids Surf., A 360 (2010) 74–84.
[31] P.A.E. Piunno, U.J. Krull, Trends in the development of nucleic acid biosensors for medical diagnostics, Anal. Bioanal. Chem. 381 (2005) 1004–1011.
[32] Y. Wei, Q.A. Huang, M.G. Li, X.J. Huang, B. Fang, L. Wang, CeO_2 nanoparticles decorated multi-walled carbon nanotubes for electrochemical determination of guanine and adenine, Electrochim. Acta 56 (2011) 8571–8575.
[33] J.S. Song, H.S. Shin, C. Kang, A carbon nanotube layered electrode for the construction of the wired bilirubin oxidase oxygen cathode, Electroanalysis 23 (2011) 2941–2948.
[34] J.S. Kim, J. Parkey, C. Rhodes, A. Gonzalez-Martin, Development of a biofuel cell using glucose-oxidase-and bilirubin-oxidase-based electrodes, J. Solid State Electrochem. 13 (2009) 1043–1050.
[35] H.S. Shin, C. Kang, Enhanced performance of the wired-bilirubin oxidase oxygen cathode with incorporation of carboxylated single-walled carbon nanotubes, Electrochim. Acta 115 (2014) 599–606.
[36] S. Mallakpour, A. Abdolmaleki, F. Azimi, Ultrasonic-assisted biosurface modification of multi-walled carbon nanotubes with thiamine and its influence on the properties of PVC/Tm-MWCNTs nanocomposite films, Ultrason. Sonochem. 39 (2017) 589–596.
[37] A. Abdolmaleki, S. Mallakpour, F. Azimi, Microwave and ultrasound-assisted synthesis of poly(vinyl chloride)/riboflavin modified MWCNTs: Examination of thermal, mechanical and morphology properties, Ultrason. Sonochem. 41 (2018) 27–36.
[38] M.H. Yang, B.G. Choi, H.S. Park, W.H. Hong, S.Y. Lee, T.J. Park, Development of a glucose biosensor using advanced electrode modified by nanohybrid composing chemically modified graphene and ionic liquid, Electroanalysis 22 (2010) 1223–1228.
[39] K.P. Lee, S. Komathi, N.J. Nam, A.I. Gopalan, Sulfonated polyaniline network grafted multi-wall carbon nanotubes for enzyme immobilization, direct electrochemistry and biosensing of glucose, Microchem. J. 95 (2010) 74–79.
[40] J.T. Holland, C. Lau, S. Brozik, P. Atanassov, S. Banta, Engineering of glucose oxidase for direct electron transfer via site-specific gold nanoparticle conjugation, J. Am. Chem. Soc. 133 (2011) 19262–19265.
[41] A.L. Goff, M. Holzinger, S. Cosnier, Enzymatic biosensors based on SWCNT-conducting polymer electrodes, Analyst 136 (2011) 1279–1287.
[42] D. Wang, L. Chen, Facile direct electron transfer in glucose oxidase modified electrodes, Electrochim. Acta 54 (2009) 4316–4320.
[43] S.M. Zakeeruddin, D.M. Fraser, M.-K. Nazeeruddin, M. Grätzel, Towards mediator design: characterization of tris-(4, 4′-substituted-2, 2′-bipyridine) complexes of iron (II), ruthenium (II) and osmium (II) as mediators for glucose oxidase of *Aspergillus niger* and other redox proteins, J. Electroanal. Chem. 337 (1992) 253–283.
[44] D.P. Drolet, D.M. Manuta, A.J. Lees, FT-IR and XPS study of copper (II) complexes of imidazole and benzimidazole, Inorg. Chim. Acta 146 (1988) 173–180.
[45] E. Kolek, P. Šimko, P. Šimon, A. Gatial, Confirmation of polymerisation effects of sodium chloride and its additives on acrylamide by infrared spectrometry, J. Food Nutr. Res. 46 (2007) 39–44.
[46] M.R. Guilherme, A.V. Reis, S.H. Takahashi, A.F. Rubira, J.P.A. Feitosa, E.C. Muniz, Synthesis of a novel superabsorbent hydrogel by copolymerization of acrylamide and cashew gum modified with glycidyl methacrylate, Carbohydr. Polym. 61 (2005) 464–471.
[47] N.D.M. Cordes, J.L. Walter C.S.C., Infrared and Raman spectra of heterocyclic compounds—I the infrared studies and normal vibrations of imidazole, Spectrochim. Acta, Part A 24 (1968) 237–252.
[48] C.O. Lim, J. Huang, S.J. Kim, H.S. Lee, H. Zeng, D.S. Hwang, Nanomechanics of poly (catecholamine) coatings in aqueous solutions, Angew. Chem. Int. Ed. 55 (2016) 3342–3346.
[49] B. White, S. Banerjee, S. O'Brien, N.J. Turro, I.P. Herman, Zeta-potential measurements of surfactant-wrapped individual single-walled carbon nanotubes, J. Phys. Chem. C 111 (2007) 13684–13690.
[50] S. Foillard, G. Zuber, E. Doris, Polyethylenimine–carbon nanotube nanohybrids for siRNA-mediated gene silencing at cellular level, Nanoscale 3 (2011) 1461–1464.
[51] J.B. Lee, S.J. Park, Y.K. Moon, S.H. Kim, K.N. Koh, Controlled thin layer coating of carbon nanotube-polymer composites for UV-visible light protection, Korean J. Chem. Eng. 26 (2009) 1790–1794.
[52] S. Costa, E. Borowiak-Palen, M. Kruszynska, A. Bachmatiuk, R.J. Malenczuk, Characterization of carbon nanotubes by Raman spectroscopy, Mater. Sci.-Poland 26 (2008) 433–441.
[53] H. Qi, J. Liu, E. Mäder, Smart cellulose fibers coated with carbon nanotubes networks, Fibers 2 (2014) 295–307.
[54] E. Mazzotta, S. Rella, A. Turco, C. Malitesta, XPS in development of chemical sensors, RSC Adv. 5 (2015) 83164–83186.
[55] T.C. Huang, L.C. Yeh, G.H. Lai, T.I. Yang, Y.J. Huang, A.Y. Lo, J.M. Yeh, Electroactive polyurea/CNT composite-based electrode for detection of vitamin C, eXPRESS Polym. Lett. 10 (2016) 450–461.
[56] R.K. Singh, R. Devivaraprasad, T. Kar, A. Chakraborty, M. Neergat, Electrochemical impedance spectroscopy of oxygen reduction reaction (ORR) in a rotating disk electrode configuration: effect of ionomer content and carbon-support, J. Electrochem. Soc. 162 (2015) F489–F498.
[57] Y. Zhang, R. Yuan, Y. Chai, Y. Xiang, C. Hong, X. Ran, An amperometric hydrogen peroxide biosensor based on the immobilization of HRP on multi-walled carbon nanotubes/electro-copolymerized nano-Pt-poly (neutral red) composite membrane, Biochem. Eng. J. 51 (2010) 102–109.
[58] X. Lu, J. Zhou, W. Lu, Q. Liu, J. Li, Carbon nanofiber-based composites for the construction of mediator-free biosensors, Biosens. Bioelectr. 23 (2008) 1236–1243.
[59] B. Unnikrishnan, S. Palanisamy, S.M. Chen, A simple electrochemical approach to fabricate a glucose biosensor based on graphene–glucose oxidase biocomposite, Biosens. Bioelectron. 39 (2013) 70–75.